

# Crystal structure and magnetic properties of (1-x)BiFeO<sub>3</sub> – xBaTiO<sub>3</sub> ceramics across the phase boundary

D.V. Zhaludkevich<sup>1\*</sup>, S.I. Latushka<sup>1</sup>, T.V. Latushka<sup>2</sup>, A.V. Sysa<sup>3,4</sup>, Yu.P. Shaman<sup>3,4</sup>,  
D.A. Dronova<sup>3</sup>, A.N. Chobot<sup>1</sup>, G.M. Chobot<sup>5</sup>, K.N. Nekludov<sup>3</sup>, M.V. Silibin<sup>1,3,4,6</sup>,  
D.V. Karpinsky<sup>1,3</sup>

<sup>1</sup> Scientific-Practical Materials Research Centre of NAS of Belarus, 220072 Minsk, Belarus

<sup>2</sup> Belarusian State Medical University, 220116 Minsk, Belarus

<sup>3</sup> National Research University of Electronic Technology "MIET", 124498 Zelenograd, Moscow, Russia

<sup>4</sup> Scientific-Manufacturing Complex "Technological Centre", 124498 Zelenograd, Moscow, Russia

<sup>5</sup> Belarusian State Agrarian Technical University 220023 Minsk, Belarus

<sup>6</sup> Institute for Bionic Technologies and Engineering, I.M. Sechenov First Moscow State Medical University, 119991 Moscow, Russia

\*Corresponding author, e-mail address: [jeludkevichdima@gmail.com](mailto:jeludkevichdima@gmail.com)

Received 7 May 2020; accepted 21 May 2020; published online 10 June 2020

## ABSTRACT

The crystal structure and magnetic properties of lead-free ceramics (1-x)BiFeO<sub>3</sub> - xBaTiO<sub>3</sub> (x < 0.40) prepared by solid state reaction method were studied depending on the chemical composition and temperature. An increase in the concentration of barium and titanium ions leads to the structural transition from the polar rhombohedral structure to the cubic structure through the phase coexistence region characterized by a formation of pseudocubic phase. The isothermal magnetization measurements indicate nearly linear field dependences of magnetization in the temperature range 5 - 300 K which corresponds to a dominance of antiferromagnetic structure in the compounds with x < 0.3. Negligible value of remnant magnetization observed for the compounds having dominant rhombohedral structure diminishes in the compounds with (pseudo) cubic structure. The correlation between the type of structural distortion and magnetic structure is discussed based on the neutron and X-ray diffraction data as well as the magnetization measurements.

## 1. INTRODUCTION

Materials based on bismuth ferrite attract great attention of the scientific community due to wide variety of structural and magnetic phase transitions [1-10]. While solid solutions based on bismuth ferrite have significant disadvantages - low residual magnetization, high conductivity, small magnitude of magnetoelectric interaction, which significantly limit the scope of their possible applications [8,11-14]. Some of these disadvantages can be overcome using various chemical doping schemes. Thus, chemical

substitution of bismuth ions by alkaline-earth elements and substitution of iron ions by other transition metals elements can be used as an effective tool for controlled changes of crystal structure and functional properties [14-19]. The use of alkaline earth ions as dopant ions leads to a significant change in the crystal structure of the compounds, thus the substitution of Ba<sup>2+</sup> ions having ionic radius larger than that of Bi<sup>3+</sup> ions causes a stabilization of cubic structure through an intermediate phases [1, 3, 20, 21].

Simultaneous substitution of perovskite lattice in A- and B- positions using alkaline earth ions and transition metals respectively allows to control

58 the crystal structure of the compounds and to  
59 modify their magnetic properties. It is also  
60 possible to control the conductivity of the BiFeO<sub>3</sub>  
61 based compounds and oxygen stoichiometry  
62 associated with transport properties [22]. It is  
63 known that chemical substitution by barium ions  
64 with ions having large ionic radius increases the  
65 concentration region of structural stability of the  
66 polar rhombohedral phase, and the substitution of  
67 iron ions by titanium ions allows to control  
68 magnetic properties of the compounds [22, 23].

69 The present work is focused on the correlation  
70 between the crystal structure and magnetic  
71 properties of the compounds across the phase  
72 transition from the rhombohedral phase to the  
73 cubic phase. It is shown that utilizing the  
74 mentioned chemical doping scheme allowed to  
75 control both electric dipole and magnetic orders in  
76 the solid solutions (1-x)BiFeO<sub>3</sub> - xBaTiO<sub>3</sub>, which  
77 makes them promising materials to be used in the  
78 field of information and energy-saving  
79 technologies. The functional materials based on  
80 BiFeO<sub>3</sub> can be also used as magnetic sensors,  
81 capacitive electromagnets, magnetic memory  
82 elements, microwave filters and other devices  
83 which do not require constant electric currents  
84 and associated heat loss.

## 85 2. EXPERIMENTAL

86 Ceramic samples of Bi<sub>(1-x)</sub>Ba<sub>x</sub>Fe<sub>(1-x)</sub>Ti<sub>x</sub>O<sub>3</sub> system  
87 with concentrations of the dopant ions in the

88 range  $0.15 \leq x \leq 0.40$  were prepared by the solid-  
89 state reaction method [3,18]. High-purity oxides  
90 Bi<sub>2</sub>O<sub>3</sub>, Fe<sub>2</sub>O<sub>3</sub>, TiO<sub>2</sub> and carbonate BaCO<sub>3</sub> (Sigma-  
91 Aldrich,  $\geq 99\%$ ) taken in stoichiometric ratio were  
92 mixed using planetary ball mill (Retsch PM 200).  
93 The samples were uniaxially pressed into tablets  
94 with a diameter of 10 mm. Preliminary synthesis  
95 was performed at 900 °C, after intermittent  
96 grinding the samples were finally synthesized at  
97 temperatures 910 - 945°C (synthesis temperature  
98 was gradually increased with the dopants  
99 concentration) [22, 24]. After synthesis the  
100 samples were cooled down to room temperature  
101 with a cooling rate of 100 °C/h.

102 X-ray diffraction patterns were recorded in the  
103 2theta range of 20 - 80° with a step of 0.02° using  
104 Bruker D8 Advance and Rigaku D/MAX-B  
105 diffractometers with Cu-K $\alpha$  radiation. Neutron  
106 powder diffraction (NPD) measurements were  
107 performed using high-resolution neutron powder  
108 diffractometer FIREPOD ( $\lambda=1.7977\text{\AA}$ , E9  
109 instrument, HZB). The diffraction data were  
110 analyzed by the Rietveld method using the  
111 FullProf software [25]. Magnetization  
112 measurements were performed in magnetic fields  
113 up to 14 T using physical properties measurement  
114 system from Cryogenic Ltd.

## 115 3. RESULTS AND DISCUSSIONS

116 The refinement of the diffraction data obtained for  
117 the compounds of the system

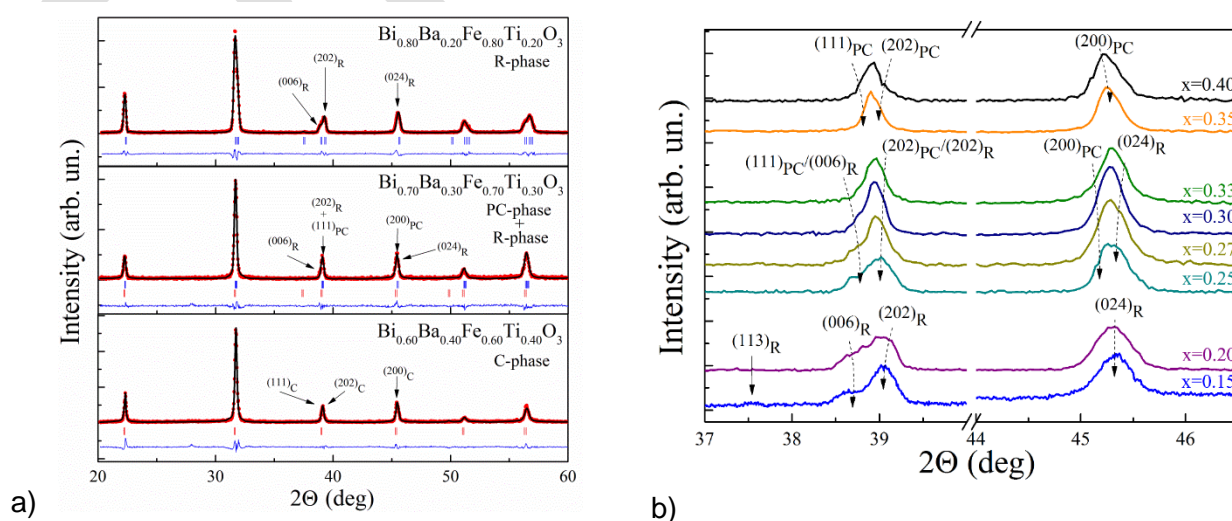


Figure 1. (a) Room-temperature XRD patterns of the compounds Bi<sub>(1-x)</sub>Ba<sub>x</sub>Fe<sub>(1-x)</sub>Ti<sub>x</sub>O<sub>3</sub> x = 0.20; 0.30; 0.40; observed and calculated profiles are marked by dots and solid line respectively, the line below the pattern refers to the difference between the profiles. The upper row of the ticks denotes Bragg reflections ascribed to the rhombohedral phase, the second row – to the cubic phase; (b) the evolution of the selected diffraction peaks depending on the concentration.

118  $\text{Bi}_{(1-x)}\text{Ba}_x\text{Fe}_{(1-x)}\text{Ti}_x\text{O}_3$  has allowed to clarify the  
 119 evolution of the crystal structure as a function of  
 120 the dopant concentration and temperature.  
 121 According to the results of the diffraction  
 122 measurements, the compounds with  $x \leq 0.2$  are  
 123 characterized by a single-phase rhombohedral  
 124 structure (Fig. 1a,b). An increase in the  
 125 concentration of the dopant content leads to a  
 126 reduction of the rhombohedral distortion, and the  
 127 structure of the compounds with  $x = 0.25 - 0.33$   
 128 can be refined assuming a coexistence of the  
 129 rhombohedral and pseudocubic phases. It should  
 130 be noted that the pseudocubic phase is observed  
 131 in the compounds  $0.25 < x < 0.40$ . This model is  
 132 in accordance with the results obtained by X-ray  
 133 and neutron diffraction measurements.

134 Chemical substitution causes gradual  
 135 decrease in rhombohedral distortions, which can  
 136 be estimated by an evolution of the reflection  
 137  $(113)_R$  (Fig. 1b) associated with a distortion of  
 138 oxygen octahedra in the  $ab$  plane of the  
 139 rhombohedral lattice. The intensity of the  
 140 reflection gradually decreases with the  
 141 concentration  $x$  and disappears for the compound  
 142  $x = 0.2$ . The splitting of the reflections  $(202)_R$  and  
 143  $(006)_R$  ( $2\theta = 39^\circ$ ) characterizing rhombohedral

145 the concentration of the dopant ions, which  
 146 indicates gradual decrease in the elongation of  
 147 the rhombohedral lattice. This splitting completely  
 148 disappears for the compound with  $x = 0.35$ , which  
 149 also confirms the absence of the rhombohedral  
 150 phase in the compounds with  $x > 0.35$ . Further  
 151 substitution leads to a transformation of the crystal  
 152 structure and the structural state becomes to be  
 153 single phase with cubic symmetry.

154 Thus, an increase in the concentration of Ba  
 155 and Ti ions in the compounds  $\text{Bi}_{(1-x)}\text{Ba}_x\text{Fe}_{(1-x)}\text{Ti}_x\text{O}_3$   
 156 leads to the structural transition from the polar  
 157 rhombohedral phase to the cubic phase through  
 158 the formation of an intermediate pseudocubic  
 159 phase. Chemical substitution leads to an increase  
 160 in the unit cell volume which is caused by larger  
 161 ionic radii of the dopant ions as compared to the  
 162 radii of Bi and Fe ions [26], wherein the  $a$ - and  $c$ -  
 163 parameters of the unit cell change in different  
 164 ways (Fig. 2). An increase in the unit cell volume  
 165 is accompanied by a gradual decrease in  
 166 rhombohedral distortion, and the angle  $\alpha_R$ , which  
 167 describes the rhombohedral distortion, gradually  
 168 increases from  $59.55^\circ$  for the compound with  $x =$   
 169  $0.2$  to  $59.98^\circ$  for the compound with  $x = 0.35$ , the  
 170 volume fraction the rhombohedral phase in the

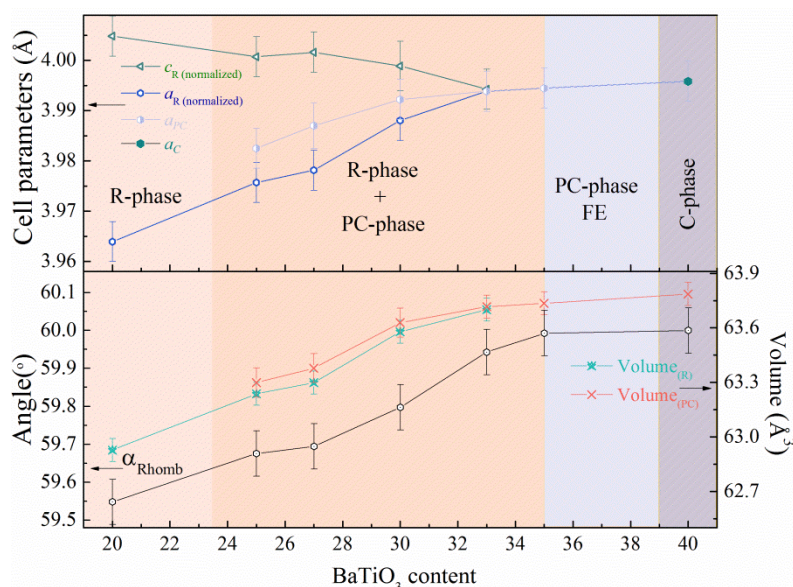


Figure 2. The dopant concentration driven evolution of the unit cell parameters (upper panel), unit cell volume of the rhombohedral and (pseudo)cubic phases and angle  $\alpha_R$  calculated for the compounds with  $0.2 \leq x \leq 0.4$ .

144 distortion gradually decreases with increasing in 171 last compound becomes to be negligible (Fig. 2).

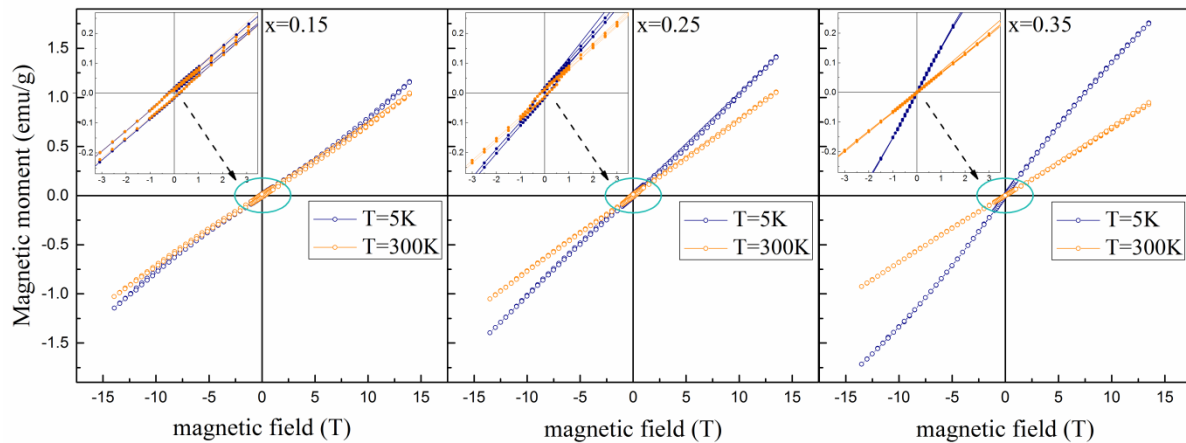


Figure 3. Field dependences of magnetization obtained for  $\text{Bi}_{(1-x)}\text{Ba}_x\text{Fe}_{(1-x)}\text{Ti}_x\text{O}_3$  compounds  $0.15 \leq x \leq 0.40$  at temperatures  $T = 5 \text{ K}$  and  $300 \text{ K}$ . The insets show magnified parts of the magnetization curves near the origin.

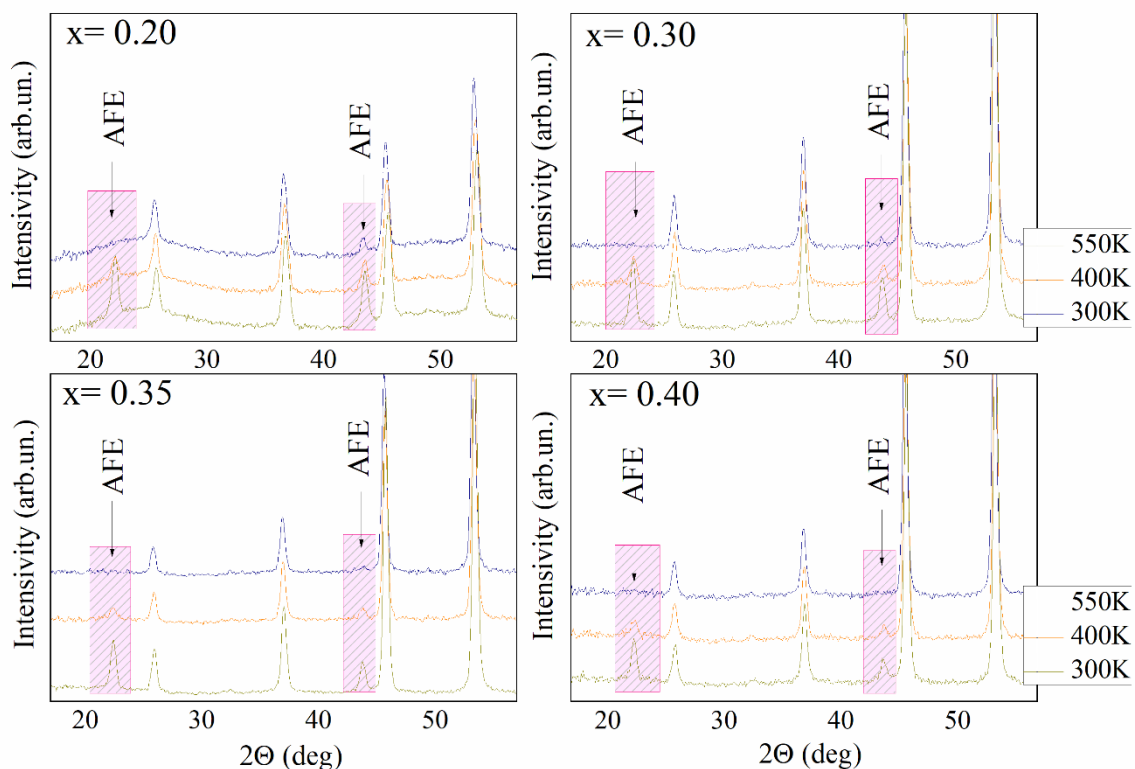


Figure 4. Temperature evolution of characteristic diffraction peaks obtained by neutron diffraction for the compounds  $\text{Bi}_{1-x}\text{Ba}_x\text{Fe}_{1-x}\text{Ti}_x\text{O}_3$  with  $0.20 \leq x \leq 0.40$ . The diffraction reflections ascribed to magnetic scattering are marked and highlighted by dashed areas.

172 It should also be noted that the parameter  $a$ -  
 173 gradually increases with the dopant content up to  
 174  $x = 0.40$ , while  $c$  - parameter begins to  
 175 significantly decrease only in the compounds with  
 176  $x = 0.27$ . It should be noted that the  $c / a$  ratio

177 which denotes polar distortion of the lattice  
 178 decreases down to unity in the compound with  $x =$   
 179  $0.33$ .

180 Magnetization measurements have allowed to  
 181 reveal a close correlation between the crystal

182 structure and magnetic properties of the  
183 compounds. The  $M(H)$  dependence obtained for  
184 the compound with  $x = 0.15$  has a residual  
185 magnetization of about 0.011 emu/g (Fig. 3, inset)  
186 and has slightly non-linear character distinctly  
187 observed at low temperature which points at a  
188 disruption of spatially modulated spin structure at  
189 high magnetic fields. The  $M(H)$  dependences  
190 obtained for compounds with the dopant content  
191  $x > 0.15$  are characterized by nearly linear  
192 character of magnetization denoting dominant  
193 antiferromagnetic structure. At  $x = 0.25$ , the  
194 compound is characterized by a mixture of  
195 dominant rhombohedral phase and minor pseudo-  
196 cubic phase and the remanent magnetization is  
197 still present with a value of about 0.014 emu/g.  
198 Increase in the concentration of the dopant ions  
199 up to  $x = 0.30$  leads to a complete collapse of  
200 remanent magnetization which is valid for the  
201 compounds with  $x \leq 0.4$ . Such evolution of  
202 magnetization is caused by a change in symmetry  
203 of the crystal structure from the rhombohedral to  
204 the (pseudo)cubic phase. Magnetization data  
205 obtained at room temperature indicate the stability  
206 of the antiferromagnetic structure in the studied  
207 temperature range and the data are in good  
208 agreement with the results obtained by the  
209 neutron diffraction measurements.

210 The results of the magnetization  
211 measurements performed for the compounds  $\text{Bi}_{(1-x)}\text{Ba}_x\text{Fe}_{(1-x)}\text{Ti}_x\text{O}_3$   
212 indicate predominantly  
213 antiferromagnetic character of the magnetic  
214 structure, which is confirmed by the results of  
215 neutron diffraction measurements which indicate  
216 the G-type antiferromagnetic structure. Analyzing  
217 the data of the neutron diffraction measurements  
218 (Fig. 4), it can be stated that the G-type  
219 antiferromagnetic structure is stable in the  
220 compounds with  $0.15 \leq x \leq 0.4$  in the temperature  
221 range  $5 \text{ K} \leq T \leq T_N$ . At temperatures above room  
222 temperature the diffraction peaks attributed to  
223 magnetic scattering become to decrease rapidly  
224 till they disappear completely at  $T_N \sim 500 \text{ K}$  for the  
225 compounds with  $x = 0.25 - 0.30$ . Increase in the  
226 dopant concentration up to  $x = 0.40$  leads a  
227 reduction of the magnetic transition temperature  
228 down to  $T_N \sim 450 \text{ K}$ .

229 Neutron diffraction data points at G-type  
230 antiferromagnetic structure which is stable in the  
231 compounds  $\text{Bi}_{(1-x)}\text{Ba}_x\text{Fe}_{(1-x)}\text{Ti}_x\text{O}_3$   $x \leq 0.40$ . The

232 magnetic moment calculated per iron ion of the  
233 compound with  $x = 0.15$  at room temperature is  
234 about  $4.5 \mu_B$  which is only a bit lower than “spin  
235 only” value of the magnetic moment estimated for  
236 the iron ions being in 3+ oxidative state ( $t_{2g}^5$ ). The  
237 nearly collinear antiferromagnetic structure  
238 remains in the compounds upon increase in the  
239 dopant content while the magnetic moment  
240 associated with the iron ions gradually decreases  
241 with  $x$ . The compound with the dopant content  
242  $x = 0.25$  is characterized by the magnetic moment  
243 of  $\sim 4.2 \mu_B$ , for the compound with  $x = 0.35$  the  
244 calculated value of the magnetic moment is  $\sim 2.9$   
245  $\mu_B$ . The obtained results are in accordance with  
246 the model of diamagnetic dilution of the  
247 magnetically active sublattice formed by the iron  
248 ions being in 3+ oxidative state, while non-  
249 magnetic titanium ions are characterized by the  
250 oxidative state of 4+. It should be noted that the  
251 remanent magnetization observed in the  
252 compounds having dominant rhombohedral phase  
253 diminishes in the compounds having dominant  
254 (pseudo) cubic phase. This observation is in  
255 accordance with the symmetry restrictions, as  
256 antisymmetric exchange interactions leading to  
257 nonzero remanent magnetization in the  
258 compounds with rhombohedral structure are  
259 forbidden in the compounds having cubic phase  
260 [27-29].

#### 261 4. CONCLUSIONS

262 The results of diffraction measurements indicate  
263 that the single-phase rhombohedral structure is  
264 stable in the compounds up to  $x = 0.2$ . An  
265 increase in the concentration of the dopant  
266 content leads to a gradual reduction of the  
267 rhombohedral distortion, the structure of the  
268 compounds with  $x = 0.25 - 0.33$  can be refined  
269 assuming a coexistence of the rhombohedral and  
270 pseudocubic phases, further increase in the  
271 dopant content leads to the phase transition to  
272 single phase cubic structure. Analysis of the  
273 isothermal dependences of the magnetization as  
274 well as neutron diffraction measurements points at  
275 G-type antiferromagnetic structure which is stable  
276 in the compounds with  $0.15 \leq x \leq 0.4$  in the wide  
277 temperature range in spite of magnetic dilution  
278 caused by Ti ions residing in the B-site of  
279 perovskite lattice. The obtained results point at

280 strong correlation between the presence of  
281 remanent magnetization and structural state of the  
282 compounds, thus confirming weak  
283 ferromagnetism specific for the compounds  
284 having rhombohedral structure; the absence of  
285 remanent magnetization in the compounds having  
286 (pseudo) cubic structure is in accordance with  
287 symmetry restrictions.

## 288 ACKNOWLEDGMENTS

289 This work was supported by the Russian Science  
290 Foundation (project 18-19-00307). The authors  
291 acknowledge HZB for the allocation of neutron  
292 radiation beamtime and HZB staff for the  
293 assistance with neutron diffraction experiments.  
294 M.S. acknowledges Russian academic excellence  
295 project "5-100" for Sechenov University.

## 296 REFERENCES

- 297 [1] [S. Kim, G.P. Khanal, H.-W. Nam, I. Fujii, S. Ueno, C. Moriyoshi, Y. Kuroiwa, S. Wada, \*J. Appl. Phys.\* \*\*122\*\*, 164105 \(2017\).](#)
- 298 [2] [R. Haumont, I.A. Kornev, S. Lisenkov, L. Bellaiche, J. Kreisel, B. Dkhil, \*Phys. Rev. B\* \*\*78\*\*, 134108 \(2008\).](#)
- 299 [3] [D.V. Karpinsky, I.O. Troyanchuk, M. Tovar, V. Sikolenko, V. Efimov, E. Efimova, V. Ya Shur, A.L. Kholkin, \*J. Am. Ceram. Soc.\* \*\*97\*\*, 2631-2638 \(2014\).](#)
- 300 [4] [D. Wang, G. Wang, S. Murakami, Z. Fan, A. Feteira, D. Zhou, S. Sun, Q. Zhao, I.M. Reaney, \*J. Adv. Dielectr.\* \*\*08\*\*, 1830004 \(35p\) \(2018\).](#)
- 301 [5] [D.C. Arnold, K.S. Knight, G. Catalan, S.A.T. Redfern, J.F. Scott, P. Lightfoot, F.D. Morrison, \*Adv. Funct. Mater.\* \*\*20\*\*, 2116-2123 \(2010\).](#)
- 302 [6] [A. Kirsch, M.M. Murshed, M.J. Kirkham, A. Huq, F.J. Litterst, T.M. Gesing, \*J. Phys. Chem. C\* \*\*122\*\*, 28280-28291 \(2018\).](#)
- 303 [7] [D. Wang, A. Khesro, S. Murakami, A. Feteira, Q. Zhao, I.M. Reaney, \*J. Eur. Ceram. Soc.\* \*\*37\*\*, 1857-1860 \(2017\).](#)
- 304 [8] [G. Catalan, J.F. Scott, \*Adv. Mater.\* \*\*21\*\*, 2463-2485 \(2009\).](#)
- 305 [9] [S.M. Selbach, T. Tybell, M.-A. Einarsrud, T. Grande, \*Adv. Mater.\* \*\*20\*\*, 3692-3696 \(2008\).](#)
- 306 [10] [D.V. Karpinsky, I.O. Troyanchuk, O.S. Mantytskaya, V.A. Khomchenko, A.L. Kholkin, \*Solid State Commun.\* \*\*151\*\*, 1686-1689 \(2011\).](#)
- 307 [11] [I.O. Troyanchuk, D.V. Karpinsky, M.V. Bushinsky, V.A. Khomchenko, G.N. Kakazei, J.P. Araujo, M. Tovar, V. Sikolenko, V. Efimov, A.L. Kholkin, \*Phys. Rev. B\* \*\*83\*\*, 054 109 \(2011\).](#)
- 308 [12] [G. Le Bras, P. Bonville, D. Colson, A. Forget, N. Genand- Riondet, R. Tourbot. \*Physica B\* \*\*406\*\*, 1492-1495 \(2011\).](#)
- 309 [13] [I. Levin, M.G. Tucker, H. Wu, V. Provenzano, C.L. Dennis, S. Karimi, T. Comyn, T. Stevenson, R.I. Smith, I.M. Reaney. \*Chem. Mater.\* \*\*23\*\*, 2166-2175 \(2011\).](#)
- 310 [14] [D. Kan, L. Palova, V. Anbusathaiah, C.J. Cheng, S. Fujino, V. Nagarajan, K.M. Rabe, I. Takeuchi. \*Adv. Funct. Mater.\* \*\*20\*\*, 1108-1115 \(2010\).](#)
- 311 [15] [D. Arnold, \*IEEE Trans. Ultrason. Ferroelectr. Freq. Control\* \*\*62\*\*, 62-82 \(2015\).](#)
- 312 [16] [D.V. Karpinsky, I.O. Troyanchuk, N.V. Pushkarev, A. Dziaugys, V. Sikolenko, V. Efimov, A.L. Kholkin, \*J. Alloy. Comp.\* \*\*638\*\*, 429434 \(2015\).](#)
- 313 [17] [V.A. Khomchenko, M.S. Ivanov, D.V. Karpinsky, J.A. Paixao, \*J. Appl. Phys.\* \*\*122\*\*, 124103 \(2017\).](#)
- 314 [18] [D.V. Karpinsky, M.V. Silibin, A.V. Trukhanov, A.L. Zhaludkevich, T. Maniecki, W. Maniukiewicz, V. Sikolenko, J.A. Paixao, V.A. Khomchenko, \*J. Phys. Chem. Solids\* \*\*126\*\*, 164-169 \(2019\).](#)
- 315 [19] [L.H. Yin, W.H. Song, X.L. Jiao, W.B. Wu, X.B. Zhu, Z.R. Yang, J.M. Dai, R.L. Zhang, Y.P. Sun, \*J. Phys. D Appl. Phys.\* \*\*42\*\*, 205402 \(2009\).](#)
- 316 [20] [A. Singh, C. Moriyoshi, Y. Kuroiwa, D. Pandey, \*Phys. Rev. B\* \*\*88\*\*, 024113 \(2013\).](#)
- 317 [21] [I. Calisir, A.A. Amirov, A.K. Kleppe, D.A. Hall, \*J. Mater. Chem. A\* \*\*6\*\*, 5378-5397 \(2018\).](#)
- 318 [22] [D.V. Karpinsky, M.V. Silibin, A.V. Trukhanov, A.L. Zhaludkevich, S.I. Latushka, D. V. Zhaludkevich, V. Sikolenko, V.A. Khomchenko, \*J. Alloy. Comp.\* \*\*803\*\*, 1136-1140 \(2019\).](#)
- 319 [23] [V.A. Khomchenko, D.V. Karpinsky, D.V. Zhaludkevich, S.I. Latushka et. al., \*Mater. Lett.\* \*\*254\*\*, 305 \(2019\).](#)
- 320 [24] [Y.P. Wang, L. Zhou, M.F. Zhang, X.Y. Chen, J.-M. Liu, Z.G. Liu, \*Appl. Phys. Lett.\* \*\*84\*\*,\) 1731 \(2004\).](#)
- 321 [25] [J. Rodríguez-Carvajal, \*Physica B\* \*\*192\*\*, 55-69 \(1993\).](#)
- 322 [26] [R. D. Shannon, \*Acta. Cryst.\* \*\*A32\*\*, 751-767 \(1976\).](#)
- 323 [27] [I. Dzyaloshinsky, \*J. Phys. Chem. Solids\* \*\*4\*\*, 241-255 \(1958\).](#)
- 324 [28] [T. Moriya, \*Phys. Rev. Lett.\* \*\*4\*\*, 228 \(1960\).](#)
- 325 [29] [T. Moriya, \*Phys. Rev.\* \*\*120\*\*, 91 \(1960\).](#)
- 326  
327  
328  
329  
330  
331  
332  
333  
334  
335  
336  
337  
338  
339  
340  
341  
342  
343  
344  
345  
346  
347  
348  
349  
350  
351  
352  
353  
354  
355  
356  
357  
358  
359  
360  
361  
362  
363  
364  
365  
366  
367  
368  
369  
370  
371  
372  
373

374  
375  
376  
377